

- (163) D. B. Gammack, *Biochem. J.*, **98**, 18P(1966).  
(164) G. Eiserman, J. P. Sandblom, and J. L. Walker, *Science*, **155**, 965(1967).  
(165) F. De Kőrosy, *Nature*, **197**, 685(1963).  
(166) C. Botrė, S. Borghi, and M. Marchetti, *Biochim. Biophys. Acta*, **135**, 162(1967).

#### ACKNOWLEDGMENTS AND ADDRESSES

Received from the *School of Pharmacy, Medical College of Virginia, Richmond, VA 23219*

The author thanks Dr. A. N. Martin for his help in the preparation of this manuscript.

## RESEARCH ARTICLES

---

# Interfacial Barriers in Interphase Transport: Retardation of the Transport of Diethylphthalate Across the Hexadecane-Water Interface by an Adsorbed Gelatin Film

ABDEL-HALIM GHANEM, W. I. HIGUCHI, and A. P. SIMONELLI

**Abstract** □ In order to investigate the possible influence of an adsorbing substance upon the oil-water interphase transport rate of a solute, experiments were conducted on the rate of release of diethylphthalate from hexadecane droplets dispersed in an aqueous sodium sulfate solution. It was found that when an adsorbed layer of gelatin is presented, the rates of solute release are the order of  $1 \times 10^4$  times slower than diffusion controlled. The permeability coefficient for the interfacial barrier was estimated to be  $1.5 \times 10^{-6} \pm 0.3$ . These findings are, to the authors' knowledge, the first of their kind, and suggest the possible importance of such nonspecific barriers in biopharmaceutics. The data have been critically analyzed by several physical models that relate the interphase transport rate to the partition coefficient, the diffusion coefficient in the aqueous phase, the particle-size distribution of the droplets, the interfacial resistance of the gelatin layer, and the adsorption of the solute to the interface. The analysis has shown that under certain conditions adsorption of diethylphthalate at the interface must be accounted for to provide quantitative agreement of the theory with the data.

**Keyphrases** □ Interphase transport—diethylphthalate □ Interfacial barrier—hexadecane-water □ Gelatin, adsorbed layer—interfacial barrier □ Particle-size distribution—emulsion systems □ Partition coefficients (o/w)—diethylphthalate □ UV spectrophotometry—analysis

An understanding of the influence of interfacially adsorbing agents on the transport-rate behavior of drugs across oil-water interfaces is basic to the understanding of drug dynamics in man. When meaningful mechanistic analyses are sought, there are many instances where the interphase transport of a drug must be considered after its administration to the patient. Cases in point are, for example, drug-release situations involving availability, drug absorption, distribution in tissues and in various body fluids, metabolism, or excretion. Hence, the question of the influence of substances adsorbed at the interface becomes an important one.

A survey of the literature has shown that very little is known about the oil-water situation. The classic work of LaMer and his collaborators (1) has given an excellent example of the air-water case. These workers found that long-chain aliphatic alcohols significantly reduced the evaporation rate of water by providing a condensed monolayer. The adsorbed layers, in these instances, create sufficiently large barriers against the movement of water molecules through them. Another case of transport-rate reduction by interfacial adsorption is the marked reduction in the dissolution rate of hydroxyapatite by adsorbed long-chain amine hydrochlorides (2). To the authors' knowledge, however, such effects have not been clearly demonstrated for the oil-water interface case.

Recently (3) a well-defined method for measuring the oil-to-water interphase transport rate was described. It involves the use of dispersed oil droplets as a sink or source for the solute in the aqueous external phase. As was pointed out (3), this technique is generally much more sensitive and more reliable than most methods for studying interfacial barrier to interphase transport.

In this communication, this technique has been applied to the investigation of the influence of gelatin adsorbed at the oil-water interface upon the transport rate of an organic solute. The present findings, to the writers' knowledge, represent the first definitive demonstration of a significant retardation of the oil-water interphase transport rate by a reversibly adsorbed substance. These results should be generally important to the eventual understanding of the role of proteins and other polymeric substances on the transport of drugs and other physiologically important substances *in vitro* and *in vivo*.

## EXPERIMENTAL

**Consideration in Design of the Experiment**—The technique basically involves following either the transfer-in of a solute from the aqueous phase to the oil droplets or the transfer-out of the solute from the oil droplets into the aqueous phase. In selecting a suitable system for a meaningful quantitative study of such a complex problem, it is very important to keep in mind the many factors that may limit the feasibility of the experiment. Thus a judicious experimental design is critical for successful study.

The system selected for the present studies was hexadecane droplets-in-water, with gelatin being the interfacially adsorbed substance. This system was chosen for the transport studies because (a) preliminary experiments had shown that a significant interfacial barrier was present; (b) a concentrated oil-in-water emulsion of this system could be conveniently prepared that was well-dispersed as single droplets and stable in other respects; (c) the size distributions of the droplets were in ranges convenient for determination by the Coulter counter; and (d) suitable solutes were available for the studies with convenient partition coefficients, oil and water solubilities, chemical stability, and general compatibility.

Furthermore, this system offered other advantages. The interfacial binding of the primary solute investigated, diethylphthalate, was relatively small compared to the amounts distributed in the oil and water phases. Thus good base line studies were anticipated.

Also gelatin distributes primarily at the interface when the electrolyte concentrations in the aqueous phase are sufficiently high. Therefore the importance of the gelatin movement in the problem is negligible.

In addition, it was believed that the hexadecane-gelatin-water interface should be of basic interest to biological situations. Later studies are planned with lipid-protein interaction barriers. The present system may then represent the primitive model for more biologically realistic barriers.

**Preparation of the System**—The hexadecane<sup>1</sup>-in-water emulsions containing diethylphthalate<sup>2</sup> as the drug were prepared in the following manner, using gelatin<sup>3</sup> as an emulsifying agent. First, a 10% gelatin solution in water was prepared by dissolving 5 g. of the gelatin in 45 g. of water at 50°. Then 20 g. of the hexadecane solution of diethylphthalate was added to the aqueous gelatin solution. The hexadecane was purified (4) and the diethylphthalate was used without further purification. The mixture was emulsified at about 50° using a blender.<sup>4</sup> The droplet particle-size distribution was controlled by emulsifying for predetermined times. A coarse emulsion resulted, for example, when the mixture was emulsified for less than 1 min. A finer emulsion was obtained when the emulsification was carried out for longer periods.

The emulsions were then aged for about 3 hr. at 50° with continuous stirring in order to establish equilibrium (5). This was carried out in a covered water-jacketed beaker with an eccentrically placed propeller-type stirrer<sup>5</sup> rotating at 500–600 r.p.m. To provide further good mixing two baffles were placed in the beaker.

The next step in the procedure was a critical one (6). In order to obtain condensation of the gelatin only at the oil-water interface, a concentrated aqueous sodium sulfate solution was added under predetermined conditions based on studies of the equilibrium phase diagram for the system (6). Exactly 50 g. of a 14% aqueous solution of sodium sulfate at 50° was added to the above system with continued stirring. The rate of addition of the sodium sulfate solution was a critical factor. The solution was added from a buret at a rate of 1.5–2 ml./min.

After completing the addition of the sodium sulfate solution, the system was aged for 30–40 hr. at 50° to achieve equilibrium. The same stirring conditions as described above were maintained during this period. After this aging period, the temperature of the system was dropped to 35° and maintained there for at least 6–8 hr. before use in the release-rate experiments. Microscopic observations of this final emulsion system showed that the droplets were nicely deaggregated and usually in the size range 2–6  $\mu$  diameter (for System 1). Figure 1 gives a dark-field photomicrograph of a typical system used in this study.

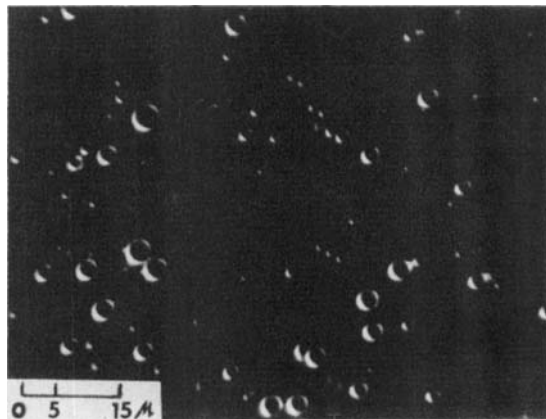


Figure 1—Dark-field photomicrograph of a typical emulsion system used in the release-rate studies.

Table I gives the final composition of the emulsion systems used in the release-rate experiments.

**Release-Rate Experiments**—In a typical release-rate experiment a predetermined amount (usually 1–6 ml.) of the above-treated emulsion system was added by means of a pipet to the release medium maintained at a constant temperature and agitation. In most of the present studies the release medium was 100 ml. of 7% aqueous sodium sulfate solution. This electrolyte concentration was selected because it was found to be high enough to prevent desorption of the gelatin from the interface but low enough so that no aggregation of the droplets was observed.

The amount released from the oil droplets to the aqueous medium was determined as a function of time. At various time intervals aliquots (usually 5 ml.) of the medium were pipeted out and filtered through a silver membrane<sup>6</sup> filter of 0.45- $\mu$  pore size and 47-mm. diameter, using the stainless steel filter funnels<sup>7</sup> under negative pressures. Generally about one-half of the sample was allowed to pass through the filter and the rest was discarded. The total time for sampling and filtration was usually around 15–20 sec.

A direct UV spectrophotometric analysis for diethylphthalate was found to be unsuitable because of the presence of gelatin. Therefore the samples were extracted with spectroquality cyclohexane<sup>8</sup> and the analysis made at  $\lambda = 273.5 \text{ m}\mu$ , using a recording spectrophotometer.<sup>9</sup>

**Particle-Size Distribution Studies**—Particle-size distribution analyses were made on all systems before and after the release-rate experiments. For this purpose a counter<sup>10</sup> with channel analyzer<sup>11</sup> was employed as was done in previous studies in these laboratories (7). For most studies the 50- $\mu$  aperture tube was used. Calibrations were made with standard latex particles.<sup>12</sup>

Figures 2 and 3 give the size-distribution data for two of the emulsion systems used in these studies and the corresponding latex-calibration data for each. The ordinate axes on the photographs refer to the number of droplets of the size indicated and the abscissas refer to the channel number which is proportional to the droplet volume. As can be seen from Figs. 2 and 3, emulsion System 1 is a coarser emulsion than System 2. The data from these photographs were directly utilized in the theoretical analyses of the release-rate data as will be discussed later.

**Partition-Coefficient Determinations**—The oil-water partition coefficients for diethylphthalate were determined in two ways: (a) without gelatin in the system and (b) with gelatin present at the oil-water interface under the same conditions as those in the solute release-rate studies. The experiments without gelatin were carried out by adding a specified volume of hexadecane containing diethylphthalate to 100 ml. of 7% sodium sulfate in a 250-ml. volumetric flask. The systems were shaken for 24 hr. in a constant-temperature

<sup>6</sup> Selas Flotronics, Spring House, Pa.

<sup>7</sup> Millipore Filter Corp., Bedford, Mass.

<sup>8</sup> Matheson Coleman and Bell, East Rutherford, N. J.

<sup>9</sup> Beckman, DK-2, Beckman Instruments, Inc., Fullerton, Calif.

<sup>10</sup> Coulter Electronics, Chicago, Ill.

<sup>11</sup> RIDL 400, Radiation Instrument Development Laboratory, Inc., Melrose Park, Ill.

<sup>12</sup> Polyvinyltoluene latex (2.051- $\mu$  diameter), Dow Chemical Co., Midland, Mich.

<sup>1</sup> Aldrich Chemical Co., Milwaukee, Wisc.

<sup>2</sup> Eastman grade, Eastman Kodak Co., Rochester, N. Y.

<sup>3</sup> Pharmagel A, Wilson's U-Cop-Co., Calumet City, Ill.

<sup>4</sup> Waring Blendor Products Corp., New York, N. Y.

<sup>5</sup> Eastern Industries, Hamden, Conn.

**Table I**—Composition of Emulsion System Used in Release-Rate Experiments

Constituent	Quantity, g.
Gelatin	5
Sodium sulfate	7
Hexadecane containing 5% diethylphthalate	20 (25.4 ml.)
Water	88
Total	120 (~121 ml.)

bath at 25°. About 15 ml. of the aqueous phase was then centrifuged to insure removal of any oil droplets and analyzed for diethylphthalate as described in the section on *Release Rates*. The partition-coefficient determinations involving gelatin were done employing a specified volume of the same emulsion systems used in the release experiments described above. The procedure was otherwise the same.

Table II shows the data obtained from various volumes of oil used. In the presence of gelatin there appears to be a slight decrease in the partition coefficient as the oil volume is increased, while without gelatin, this trend does not appear to be present within the uncertainty of the experiment. These data will be used later in the theoretical interpretation of the release-rate experiments.

### RESULTS AND DISCUSSION

The experimental data obtained for the release of diethylphthalate as a function of time were generally quite reproducible (~2-4%)

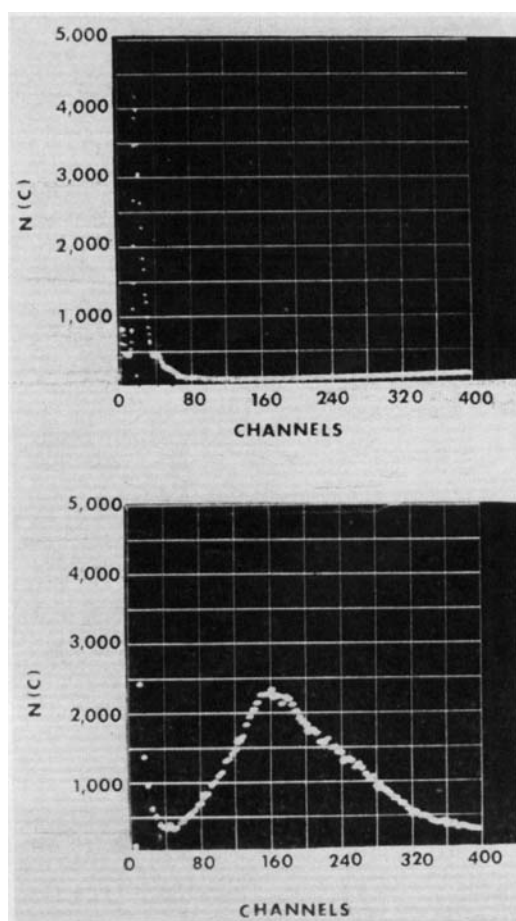


**Figure 2**—Droplet-size distribution data obtained with the Coulter counter and RIDL400 channel analyzer. Lower photograph gives data obtained with System 1. Upper photograph shows calibration data obtained with 2.051- $\mu$  diameter polyvinyltoluene latex. N(C) is the concentration of particles in Channel C.

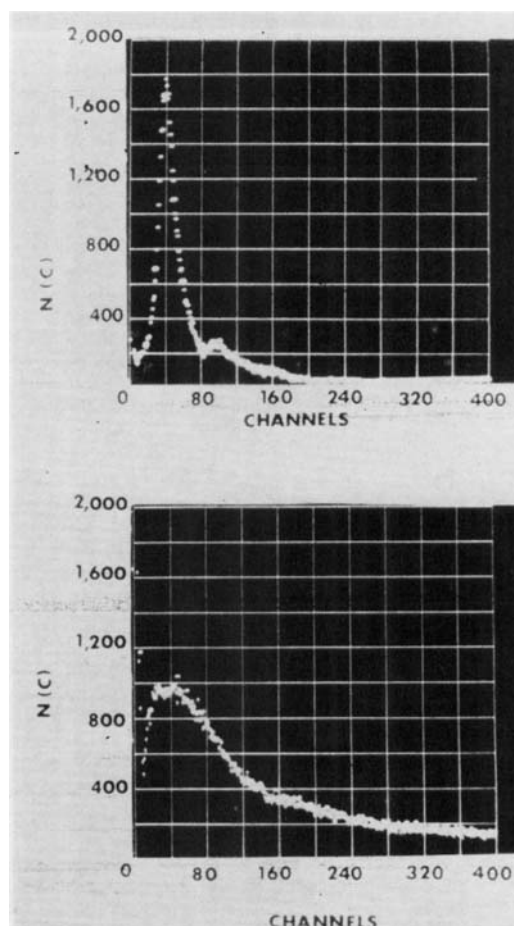


**Figure 3**—Droplet-size distribution data obtained with the Coulter counter and RIDL400 channel analyzer. Lower photograph gives data obtained with System 2. Upper photograph shows calibration data obtained with 2.051- $\mu$  diameter polyvinyltoluene latex. N(C) is the concentration of particles in Channel C.

when experiments were repeated with the same batch or with different batches prepared in the same way. This can be seen by examining Table III which shows some typical results.

Mass balance checks were made under the conditions of the release experiments by total extraction of the emulsions with cyclohexane and the recovery was always 98% or better. Furthermore, the possibility of the ester hydrolysis under the conditions of these studies was ruled out by the absence of detectable amounts of phthalic acid in the aqueous phase.

**Effect of Changing Amount of Oil Phase**—Figure 4 shows the

**Table II**—Partition Coefficient of Diethylphthalate for Hexadecane-Aqueous Sodium Sulfate 7% at 25°<sup>a</sup>

Without Gelatin		With Adsorbed Gelatin	
Volume of Oil, ml.	Partition Coefficient <sup>b</sup>	Volume of Oil, ml.	Partition Coefficient
0.08	156 ± 7.6 <sup>c</sup>	0.087	225 ± 3.2 <sup>c</sup>
0.17	155 ± 10.5	0.168	212 ± 5.3
0.34	160 ± 9.5	0.402	202 ± 5.4
0.68	159 ± 7.5	0.760	192 ± 3.5
1.32	164 ± 7.5	1.329	188 ± 1.8

<sup>a</sup> The concentration of diethylphthalate was 0.05096 ml./ml. and the aqueous medium was 100 ml. 7% (wt./wt.) sodium sulfate. <sup>b</sup> An average value was 158.6 ± 4. <sup>c</sup> Standard deviations of quadruplicate determinations.

**Table III—Release Rate of Diethylphthalate from an Emulsion System<sup>a</sup>**

System	Time, min.	Aqueous Concn., <sup>b</sup> ml./ml. $\times 10^5$				Average Aqueous Concn., ml./ml. $\times 10^5$
		I	II	III	IV	
1	0.5	1.81	1.78	1.93	1.84	1.84 $\pm$ 0.09 <sup>c</sup>
2	2.0	4.24	4.12	4.43	4.56	4.34 $\pm$ 0.20
3	5.0	7.09	6.90	6.90	6.96	6.96 $\pm$ 0.09
4	10.0	9.74	9.90	9.93	10.06	9.91 $\pm$ 0.13
5	20.0	12.05	12.05	12.21	12.34	12.16 $\pm$ 0.14
6	40.0	13.12	13.08	13.43	13.33	13.24 $\pm$ 0.17
7	100.0	13.43	13.43	13.65	13.65	13.54 $\pm$ 0.13
8	160.0	13.49	13.65	13.65	13.65	13.61 $\pm$ 0.12

<sup>a</sup> System 1, 3-ml. run, temperature 25°. <sup>b</sup> I and II were two experiments from the same emulsion. III and IV were two runs from a preparation made in the same way as that for I and II. <sup>c</sup> Standard deviations.

experimental release data when different amounts of an emulsion system were added to 7% sodium sulfate solutions. The amount of the added emulsion increases both the rate of release and the total amount released at equilibrium. By referring to the composition of the emulsion system (see Table I) it can be shown that the limiting values in Fig. 4 agree well with those predicted by the partition coefficients given in the last column of Table II.

**Influence of Medium on Release Rates**—Figure 5 shows the data obtained when water at 25° was used as the medium instead of 7% sodium sulfate. The rate of release in this case was quite rapid. When the same experiment was repeated at 50°, essentially equilibrium aqueous concentrations were obtained in about 1 min.

The difference in the height (plateau values) of the two curves was mainly due to the difference in the partition coefficient of diethylphthalate with and without sodium sulfate.

The almost instantaneous release at 50° serves to emphasize the magnitude of the adsorbed gelatin barrier. Conservative theoretical estimates for purely aqueous diffusion-controlled release (3) give approximately 0.1 sec. for the time necessary for reaching 90% of equilibrium. Therefore, the presence of the gelatin at the interface gives rise to about a 10,000-fold reduction in interphase transport.

**Influence of Temperature**—Figure 6 shows a comparison between runs made at 25° and 50°. The runs at 50° gave faster rates and somewhat higher aqueous equilibrium concentrations presumably due to a smaller apparent oil-water partition coefficient at the higher temperature.

**Effect of Particle-Size Distribution**—Figure 7 shows a comparison of runs made at 25° with two size distributions (see Figs. 2 and 3). As will be shown later, the difference in behavior may be accounted for by the proper consideration of the role of particle-size distribution in the overall transport.

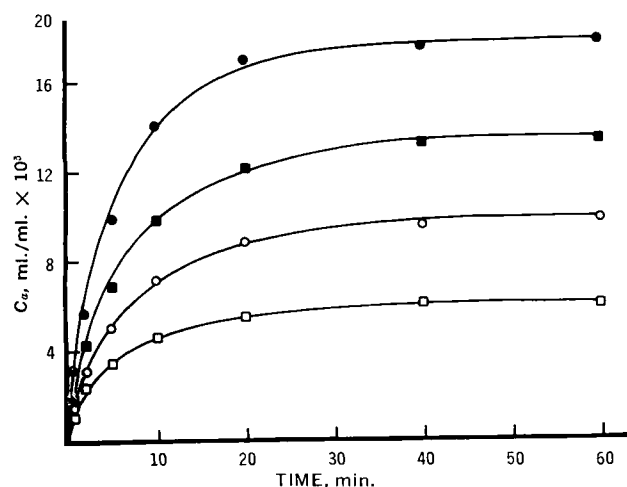


**Figure 4—Release of diethylphthalate from the emulsion System 1. Emulsion system added to 100 ml. of 7% sodium sulfate at 25°. Key:  $\square$ , 0.75 ml.;  $\circ$ , 1.5 ml.;  $\blacksquare$ , 3.0 ml.;  $\bullet$ , 6.0 ml.**

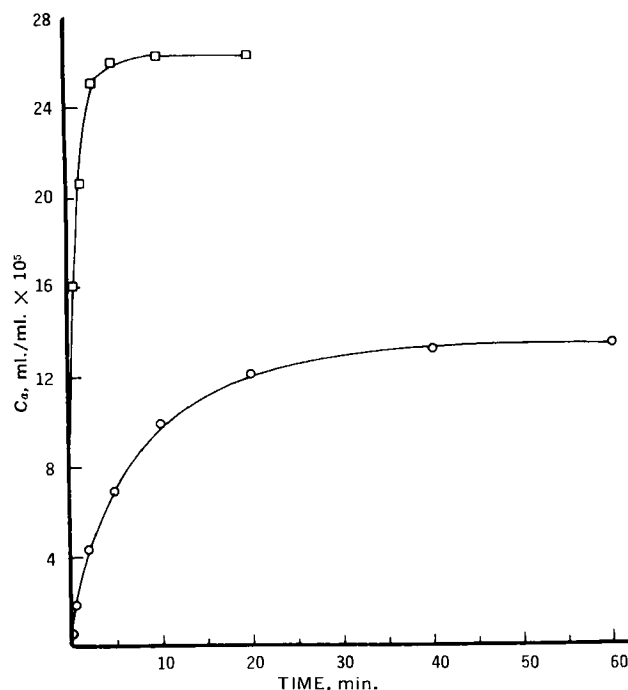


**Figure 5—Release of diethylphthalate from 3 ml. of emulsion System 1 into water at 25° ( $\circ$ ) and into 7% sodium sulfate at 25° ( $\square$ ).**

#### ANALYSES OF THE DATA WITH THEORY

In a number of respects the present experimental situation is ideal from the standpoint of theoretical analysis. First, the droplets are nonaggregated spheres. Therefore the mathematics of diffusion is simplified. Second, the adsorbed gelatin would be expected to be of uniform thickness and in a near-equilibrium state. Thus it may be appropriate to relate the permeability of such adsorbed films to equilibrium molecular configurations of polymers at the interface. Finally, the release rate and other data are of sufficiently high precision so that a critical analysis of the experiments can be made.

The basic model is shown in Fig. 8. Here the oil droplet of radius,  $a_i$ , has a gelatin-adsorbed layer.  $C_a$  and  $C_o$  are the solute concentrations in the aqueous and the oil phases, respectively, at any time after the beginning of an experiment.

The rate of solute release,  $G_i$ , from the droplet may be given by (8)

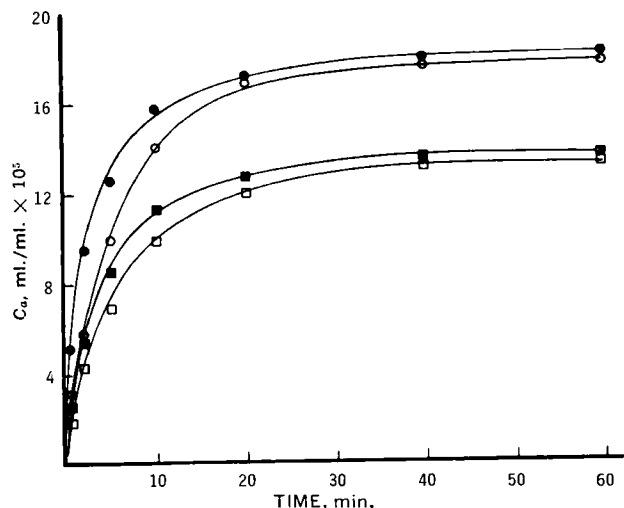


**Figure 6—Release of diethylphthalate from emulsion System 1 in 7% sodium sulfate at two different temperatures. Key:  $\square$ , 3 ml. at 25°;  $\blacksquare$ , 3 ml. at 50°;  $\circ$ , 6 ml. at 25°;  $\bullet$ , 6 ml. at 50°.**

$$G_i = 4\pi a_i D(C' - C_a) \quad (\text{Eq. 1})$$

and

$$G_i = 4\pi a_i^2 P(C_{wi} - C') \quad (\text{Eq. 2})$$

Here  $D$  is the diffusion coefficient of the solute in the aqueous phase,  $C'$  is the aqueous solute concentration just outside the adsorbed film,  $P$  is the permeability constant for the gelatin film, and  $C_{wi}$  is defined by the oil-water partition coefficient,  $K$ , as

$$K = \frac{C_{oi}}{C_{wi}} \quad (\text{Eq. 3})$$

and is the hypothetical aqueous concentration of the solute in equilibrium with  $C_{oi}$ .

Equation 2 gives the solute transport rate across the gelatin film and Eq. 1 gives the solute transport rate away from the droplet. These two rates are equal in the steady state, which is assumed in the present problem. It is also assumed that  $K$  is independent of solute concentration, *i.e.*, Henry's law is obeyed in both phases.

Equations 1 and 2 may be solved to eliminate  $C'$ . This gives

$$G_i = \frac{4\pi a_i^2 DP(C_{wi} - C_a)}{D + a_i P} \quad (\text{Eq. 4})$$

Equation 4 expresses the transport rate out of the droplet as a function of the properties of the film and the external aqueous phase.

$G_i$  may also be related to the time change in  $C_{wi}$  by

$$G_i = -KV_{oi} \frac{dC_{wi}}{dt} \quad (\text{Eq. 5})$$

Therefore, solving Eqs. 4 and 5 gives

$$-\frac{dC_{wi}}{dt} = \frac{4\pi a_i^2 DP(C_{wi} - C_a)}{KV_{oi}(D + a_i P)} \quad (\text{Eq. 6})$$

As  $V_{oi} = 4/3 \pi a_i^3$ , Eq. 6 becomes

$$-\frac{dC_{wi}}{dt} = \frac{3DP(C_{wi} - C_a)}{Ka_i(D + a_i P)} \quad (\text{Eq. 7})$$

When the total system is under consideration, one must write an equation like Eq. 7 for each size. Thus one has the set of equations

$$\left. \begin{aligned} -\frac{dC_{w1}}{dt} &= \frac{3DP(C_{w1} - C_a)}{Ka_1(D + a_1 P)} \\ -\frac{dC_{w2}}{dt} &= \frac{3DP(C_{w2} - C_a)}{Ka_2(D + a_2 P)} \\ &\vdots \\ -\frac{dC_{wL}}{dt} &= \frac{3DP(C_{wL} - C_a)}{Ka_L(D + a_L P)} \end{aligned} \right\} \quad (\text{Eq. 8})$$

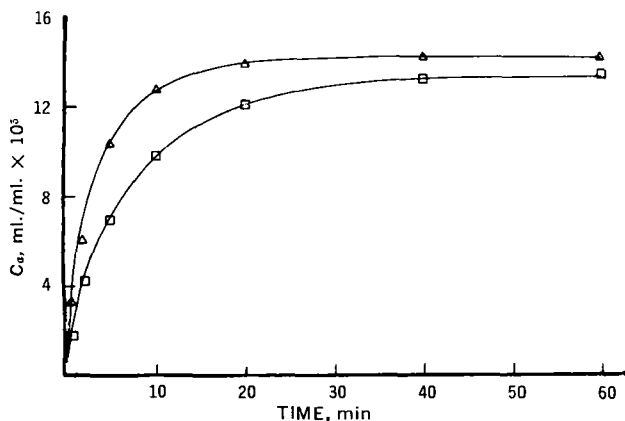


Figure 7—Release of diethylphthalate from emulsion Systems 1 and 2 in 7% sodium sulfate at 25°. Key: □, 3 ml. of System 1; △, 3 ml. of System 2.

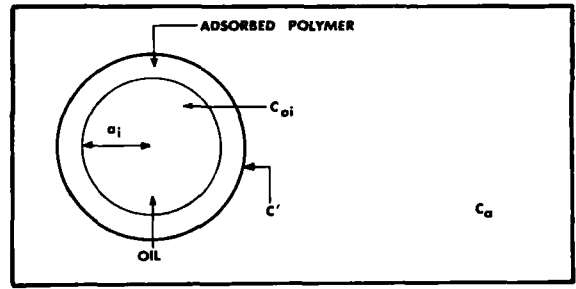


Figure 8—The physical model that describes the release of the solute (diethylphthalate) from the oil droplet to the aqueous phase. Key:  $a_i$  = droplet radius;  $C'$  = aqueous solute concentration just outside the adsorbed film;  $C_{oi}$  = solute concentration in the oil phase;  $C_a$  = solute concentration in the aqueous phase.

Here  $a_i$  and  $a_L$  represent the smallest and the largest droplets in the system.

Mass balance considerations for the total system gives

$$(C_a - E)V_a = \sum_{i=1}^L V_{oi} n_i (C_{oi}^* - C_{oi}) \quad (\text{Eq. 9})$$

Here  $V_a$  is the volume of the aqueous phase,  $E$  and  $C_{oi}^*$  are the aqueous phase and the oil phase concentrations at zero time, and  $n_i$  is the number of droplets in the system with radii between  $a_i$  and  $a_{i+1}$ . The summation in Eq. 9 is over  $a_i = a_1$  to  $a_i = a_L$ . Equation 9 simply states that the total solute lost by the oil phase must be equal to the total solute gained by the aqueous phase.

Equations 8 and 9 may be solved by numerical methods in the following manner. First, Eq. 8 may be written as a set of difference equations,

$$\left. \begin{aligned} -\Delta C_{w1} &= \frac{3DP(C_{w1} - C_a)}{Ka_1(D + a_1 P)} \Delta t \\ -\Delta C_{w2} &= \frac{3DP(C_{w2} - C_a)}{Ka_2(D + a_2 P)} \Delta t \\ &\vdots \\ -\Delta C_{wL} &= \frac{3DP(C_{wL} - C_a)}{Ka_L(D + a_L P)} \Delta t \end{aligned} \right\} \quad (\text{Eq. 10})$$

Then it can be seen that by starting  $C_a = E$  and  $C_{wi} = C_{oi}^*/K$  for  $1 \leq i \leq L$  at  $t = 0$ , one may calculate a  $\Delta C_{wi}$  for each  $i$  taking a sufficiently small  $\Delta t$ . Then one may calculate a new  $C_{wi}$  according to

$$C_{wi} = \frac{C_{oi}^*}{K} + \Delta C_{wi}$$

at  $t = \Delta t$  for each  $i$ . These values for  $C_{wi} = C_{oi}/K$  may be placed into Eq. 9 to calculate a value for  $C_a$  if the  $n_i$  values are known. Then using this new value for  $C_a$ , another set of  $\Delta C_{wi}$  values may be calculated for the second increment of time,  $\Delta t$ , and new  $C_{wi}$  values may be calculated. The calculations may be continued in this manner. Thus,  $C_a$  and  $C_{oi}$  values as functions of time may be obtained.

Such computations are best handled by digital computers.<sup>13</sup> The computer flow diagram shown in Fig. 9 was used for this purpose to calculate the  $C_a$  and  $C_{oi}$  values at different time intervals.

The particle-size distribution data (see Figs. 2 and 3) enabled the construction of a table of  $a_i, n_i$  values. Table IV gives the case where  $i$  goes from 1 to 12. This information was then employed with Eqs. 9 and 10 in the calculations.

By means of the procedure described above, four modifications of the basic model have been investigated. These have been used to analyze the experimental data, and the results are discussed in the following.

<sup>13</sup> IBM 7090 digital computer, The University of Michigan Computing Center, Ann Arbor, Mich.

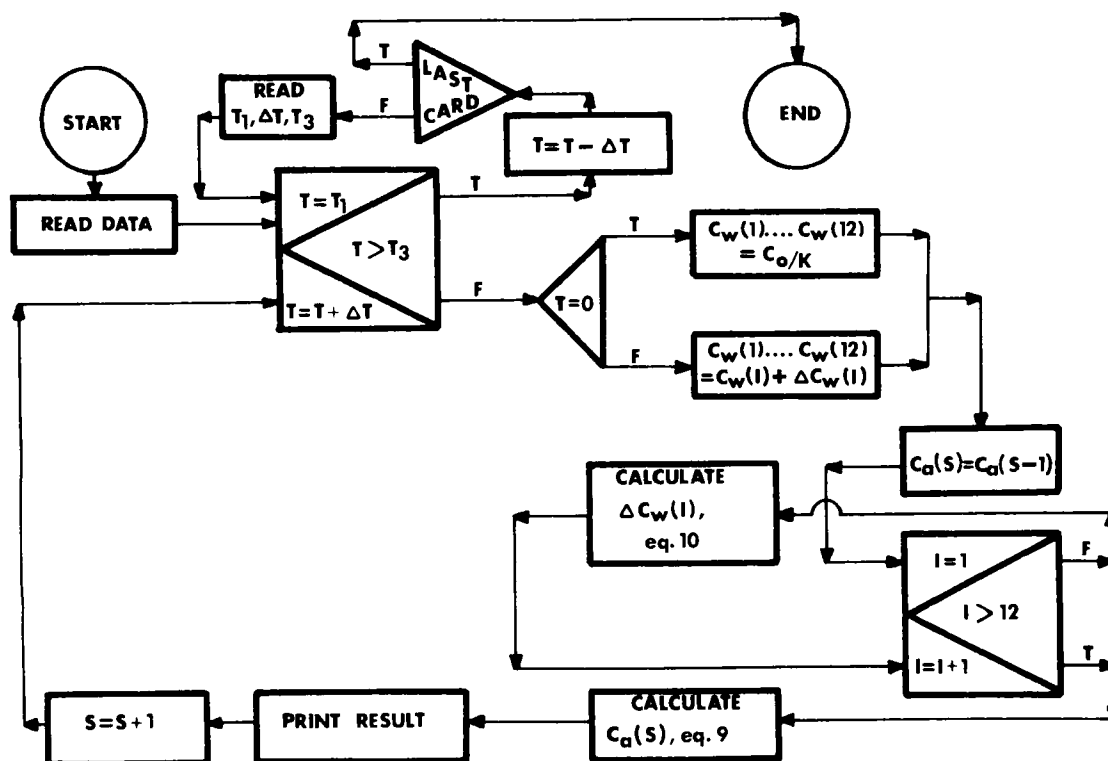


Figure 9—Flow diagram showing the procedure for computation of  $C_a$ . For Models 1 and 2 Eqs. 9 and 10 were used. For Model 3, instead of Eq. 9, Eq. 11 was used.

**Model No. 1**—The results of the theoretical computation employing the true oil-water partition coefficient value of  $K = 158.6$  (see Table V) are shown (curves) in Fig. 10 and compared to the experimental data on the oil-volume dependence. The only adjustable parameter in these calculations was the permeability constant,  $P$ . The comparisons for  $P = 1.5 \times 10^{-5}$  cm. sec.<sup>-1</sup> show that the agreement between experiment and theory is only semiquantitative. The shapes of the theoretical curves and the oil-volume dependence are not in good agreement with the experimental data. Other choices for  $P$  may improve the fit in some places but would increase the discrepancies in other places.

The relatively unsatisfactory agreement between experiment and theory found in Fig. 10 is not surprising in view of the partition-coefficient data given in Table II. The partition coefficients with adsorbed gelatin in the system are generally higher than those obtained without gelatin. Furthermore, the former shows a dependence upon the amount of the initial emulsion system added to the aqueous sodium sulfate solution.

The differences in the partition coefficients may be attributed to the binding of diethylphthalate on the adsorbed gelatin. The ratio

of the amount surface bound to that in the bulk oil appears to increase with decreasing amount of the emulsion system added to the aqueous sodium sulfate. These effects may easily account for the lack of agreement.

**Model No. 2**—Figure 11 shows the comparison between experiment and theory (Eqs. 9 and 10) using the partition-coefficient data obtained from the system containing adsorbed gelatin. In effect, this procedure amounts to fitting each theoretical curve to its long time experimental  $C_a$  value. It can be seen that the agreement between experiment and theory is much better, but this was accomplished at the expense of degrading the partition coefficient to an adjustable parameter. Even then, the shapes of the theoretical curves deviate somewhat from the experimental data.

**Model No. 3**—The analyses with both Models 1 and 2 showed that revisions in the basic equations were perhaps necessary if agreement between experiment and theory were to be achieved.

In this model the binding of diethylphthalate is explicitly included in the equations. The assumption is made that the solute bound at the interface is in rapid equilibrium with the aqueous phase. For this situation Eqs. 8 or 10 should still hold. However Eq. 9 must be

Table IV—Oil Droplet Size Distributions and Data Treatment of Emulsion Systems 1 and 2 Given in Figs. 2 and 3

$i$	Channels	System 1			System 2		
		Radius, $\mu^a$	Total No. of Particles $\times 10^{-8}$	Total Volume $\times 10^{-10}$ ( $\mu^3$ )	Radius, $\mu^a$	Total No. of Particles $\times 10^{-1}$	Total Volume $\times 10^{-10}$ ( $\mu^3$ )
1	0-40	1.03	21.75	0.98	0.81	119.15	2.69
2	40-80	1.48	7.12	0.96	1.09	111.49	6.05
3	80-120	1.75	13.84	3.13	1.29	74.16	6.70
4	120-160	1.96	27.36	8.65	1.45	49.44	6.25
5	160-200	2.13	29.00	11.80	1.57	42.02	6.84
6	200-240	2.28	20.96	10.42	1.68	30.90	6.14
7	240-280	2.41	16.35	9.60	1.77	27.44	6.45
8	280-320	2.52	10.55	7.15	1.86	24.72	6.70
9	320-360	2.64	6.26	4.81	1.94	19.78	6.08
10	360-400	2.74	4.28	3.68	2.02	17.30	5.94
11	400-440 <sup>b</sup>	2.83	2.30	2.19	2.08	11.12	4.22
12	440-480 <sup>b</sup>	2.92	.99	1.03	2.15	4.95	2.06

<sup>a</sup> Mean radius, <sup>b</sup> Obtained by extrapolation.

**Table V**—Data Used for Theoretical Computation with Models 1 and 2<sup>a</sup>

Emulsion System, Used, ml.	Oil Volume, ml.	$C_0^*$ , ml./ml.	$E \times 10^6$	$P \times 10^5$	$K^b$	$K^c$
0.75	0.161	0.05013	1.331	1.5	158.6	215
1.50	0.322	0.05011	2.662	1.5	158.6	200
3.0	0.644	0.05005	5.324	1.5	158.6	216
6.0	1.288	0.05000	10.648	1.5	158.6	200

<sup>a</sup>  $D = 6.5 \times 10^{-6}$  cm.<sup>2</sup>/sec. was used in the theoretical computations. <sup>b</sup>  $K$  values used in Model 1. <sup>c</sup>  $K$  values used in Model 2.

modified to give

$$C_a V_a + A(C_a, V_0) - E' V_a - A(E', V_0) = \sum_{i=1}^L V_{oi} n_i (C_0^* - C_{oi}) \quad (\text{Eq. 11})$$

Here  $A(C_a, V_0)$  is the amount of diethylphthalate bound and is a function of  $C_a$  and  $V_0$ , the total amount of oil for a constant-droplet-size distribution system.  $E' V_a$  represents the amount in the aqueous phase at  $t=0$  and is defined by

$$E' V_a = E V_a + Q - A(E', V_0) \quad (\text{Eq. 12})$$

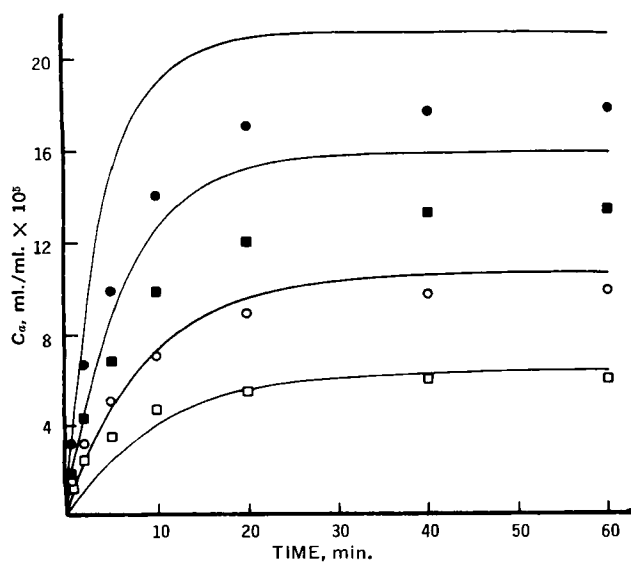
Here  $E$  is the expected aqueous concentration based on the experimental analysis of the equilibrium aqueous phase of the emulsion system prior to dilution in the 7% sodium sulfate solution.  $Q$  is the amount of diethylphthalate bound to the adsorbed gelatin in the concentrated emulsion system prior to dilution, and  $A(E', V_0)$  is the amount bound at  $E'$  when  $t=0$ .

The function,  $A(C_a, V_0)$ , may be deduced from the data on partition coefficients given in Table II. One may write the following equation

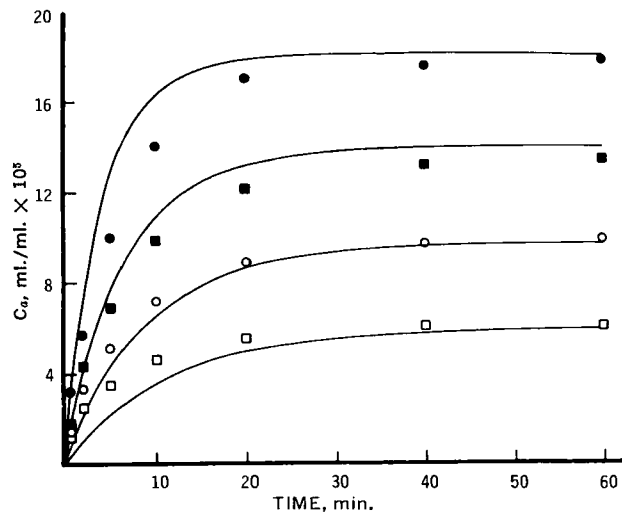
$$K' = K + \frac{A(C_a, V_0)}{V_0 C_a} \quad (\text{Eq. 13})$$

where  $K'$  is the partition coefficient in the presence of adsorbed gelatin and  $K$  is the true partition coefficient, *i.e.*, that with gelatin absent in the system. Thus one has

$$\frac{A(C_a, V_0)}{V_0} = C_a (K' - K) \quad (\text{Eq. 14})$$



**Figure 10**—Comparison of experimental data with theory using Model 1.  $C_a$  = amount of diethylphthalate released, ml./ml., versus time in minutes. Key: experimental points from System 1, □, 0.75 ml.; ○, 1.5 ml.; ■, 3.0 ml.; ●, 6.0 ml. Curves are theoretical values computed using Eqs. 9 and 10. The parameters used are shown in Tables IV and V.



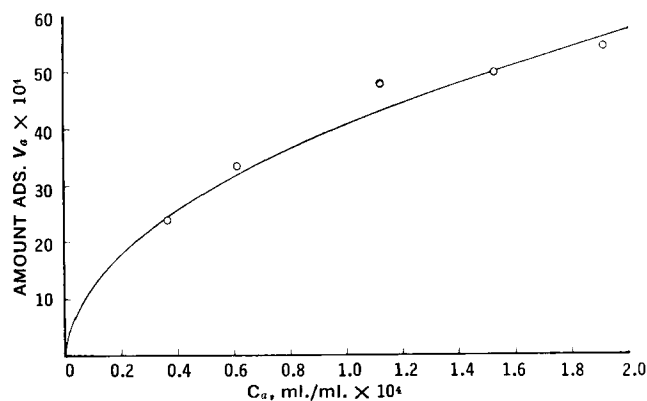
**Figure 11**—Comparison of experimental data with theory using Model 2.  $C_a$  = amount of diethylphthalate released, ml./ml., versus time in minutes. Key: experimental points from System 1, □, 0.75 ml.; ○, 1.5 ml.; ■, 3.0 ml.; ●, 6.0 ml. Curves are theoretical values computed using Eqs. 9 and 10. Parameters used are shown in Tables IV and V.

Figure 12 shows a plot of  $A(C_a, V_0)/V_0$  as a function of  $C_a$ . The experimental data on  $K'$  and  $K$  were taken from Table II. The curve in Fig. 12 is the function

$$\frac{A(C_a, V_0)}{V_0} = 0.408 C_a^{1/2} \quad (\text{Eq. 15})$$

and was obtained by treating the experimental data statistically using the least-squares method.

For the theoretical calculations with Model 3, it was decided to



**Figure 12**—Amount of diethylphthalate adsorbed per unit volume of oil phase as a function of diethylphthalate concentration in the aqueous phase. The construction of the plot is based on Eq. 14 and the experimental data shown in Table II. Key: ○, experimental data; curve is Eq. 15 used in the theoretical calculations.

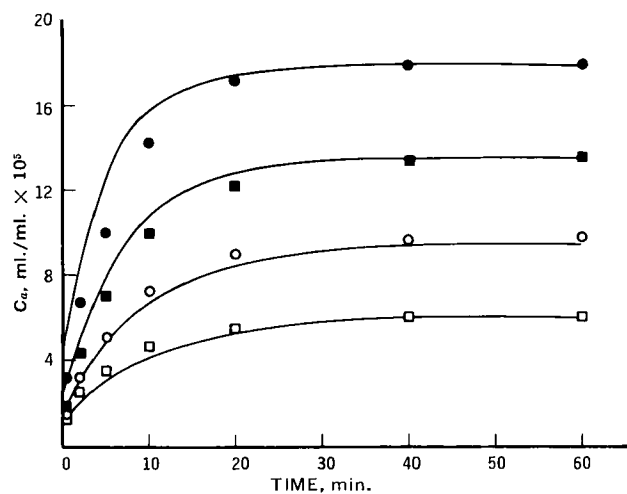


**Figure 13**—Comparison of experimental data with theory using Model 3.  $C_a$  = amount of diethylphthalate released, ml./ml., versus time in minutes. Key: experimental points from System 1, □, 0.75 ml.; ○, 1.5 ml.; ■, 3.0 ml.; ●, 6.0 ml. Curves are theoretical values computed using Eqs. 10–16. Parameters used are shown in Tables IV and VI.

use Eq. 15 for  $0 < C_a < 1.5 \times 10^{-4}$  ml./ml. and

$$\frac{A(C_a, V_0)}{V_0} = \frac{Q}{V_0} = 5.2 \times 10^{-3} \text{ ml./ml.} \quad (\text{Eq. 16})$$

Figure 13 shows the results of the theoretical calculations with Model 3. Equations 10 to 16 were used with  $K = 158.6$  and  $P = 1.5 \times 10^{-5}$ . Table VI shows  $Q$  values with  $E'$  values used for the theoretical computation with Model 3.

The agreement of the experimental data with Model 3 is very satisfactory and appears to be an improvement over the comparison of Models 1 and 2 with the data.

**Model No. 4**—Although Model 3 was found to be in very good agreement with the data, it was decided to explore the situation in which it is assumed that the bound solute is in rapid equilibrium with the solute in the oil phase rather than with that in the aqueous. As will be seen, the agreement between data and Model 4 is not as satisfactory as was the case with Model 3.

One may write for this situation

$$C_{oi}^T = C_{oi} + f(C_{oi}, a_i) \quad (\text{Eq. 17})$$

where  $C_{oi}^T$  is the apparent concentration of the solute in the oil droplet of radius,  $a_i$ , and  $f(C_{oi}, a_i)$  is the contribution to  $C_{oi}^T$  due to the bound solute, and it is a function of  $a_i$  and  $C_{oi}$ .

From geometrical considerations of a sphere, one can deduce that at equilibrium

$$f(C_{oi}, a_i) = \frac{HC_{wi}^{1/2}}{a_i} \quad (\text{Eq. 18})$$

with  $H$  as a constant if Eq. 3 is assumed and if a square-root binding relationship (see Fig. 12 and Eq. 15) is assumed. Therefore one has

$$C_{oi}^T = KC_{wi} + \frac{HC_{wi}^{1/2}}{a_i} \quad (\text{Eq. 19a})$$

for  $C_{wi} < 1.5 \times 10^{-4}$  and

$$C_{oi}^T = KC_{wi} + \frac{H(1.5 \times 10^{-4})^{1/2}}{a_i} \quad (\text{Eq. 19b})$$

for  $C_{wi} \geq 1.5 \times 10^{-4}$ .

The constant  $H$  may be evaluated in the following way. The amount of the bound solute per droplet =  $(V_{oi}HC_{wi}^{1/2})/a_i$ . Therefore the total amount of solute bound in the system is given by

$$A = \sum_{i=1}^L \frac{n_i V_{oi} H C_{wi}^{1/2}}{a_i} \quad (\text{Eq. 20})$$

whence

$$H = \frac{A}{\sum_{i=1}^L (n_i V_{oi} C_{wi}^{1/2}) a_i} = \frac{A}{\sum_{i=1}^L n_i 4/3 \pi a_i^2 C_{wi}^{1/2}} \quad (\text{Eq. 21})$$

The value for  $A$  may be taken from any point on the adsorption curve (Fig. 12) and the corresponding  $C_a$  value may be used for  $C_{wi}$ . The  $a_i$  and  $n_i$  values may be taken from the particle-size distribution data (Table IV).

It should be noted that the constant,  $H$ , is independent of the amount of the emulsion system used in the experiments, but it is dependent on the particle-size distribution for a constant oil-to-gelatin ratio. For System 1, it may be calculated that  $H = 9.63 \times 10^{-5}$  and for System 2,  $H = 6.62 \times 10^{-5}$ .

For this model instead of Eq. 10, one obtains

$$\Delta C_{oi}^T = \frac{3DP(C_{wi} - C_a)}{a_i(D + a_iP)} \cdot \Delta t \quad (\text{Eq. 22})$$

for  $1 \leq i \leq L$ .

Thus the theoretical  $C_a$  versus  $t$  plots may be constructed by numerically solving Eqs. 22, 9, 19a, and 19b. The appropriate boundary condition is that at  $t = 0$ ,  $C_{wi} = C_0^*/K$ . Table VII shows the input data for the computer.

Figure 14 shows the comparison of the same experimental data as before with Model 4. The agreement is again poorer than that obtained with Model 3, particularly the intercepts and the shapes of the curves. These negative results together with those given in Figs. 10, 11, and 13 strongly support Model 3 in which it is assumed that the bound diethylphthalate is in rapid equilibrium with the aqueous phase.

**Particle-Size Distribution Effects**—Figure 15 shows a comparison of Model 3 results with experimental data obtained employing emulsion Systems 1 and 2 (see Figs. 2 and 3 and Table IV). As can be seen, the agreement is quite good. This is further support of the general model as the particle-size distribution was the only factor different in the two theoretical calculations.

**Concentration Changes in the Oil Droplets**—Figure 16 shows the results of theoretical calculations (Model 3) for the solute concentration in the oil phase,  $C_{oi}$ , for three droplet sizes. It is seen that in this particular experiment, the smaller droplets release faster than the larger ones. Furthermore, according to theory an overshoot and a rebound occur with the smallest droplets in this system. A similar phenomenon was observed in earlier experimental studies (9) on dibutylphthalate release from hexadecane-dibutylphthalate droplets in an aqueous medium.

**Table VI**—Data Used for Theoretical Computation with Model 3<sup>a</sup>

Emulsion System Used, ml.	Oil Volume, ml.	$C_0^*$ , ml./ml.	$Q \times 10^4$	$E' \times 10^5$	$P \times 10^5$	$K$
0.75	0.161	0.04493	8.372	1.193	1.5	158.6
1.50	0.322	0.04493	16.744	1.522	1.5	158.6
3.00	0.644	0.04493	33.488	2.400	1.5	158.6
6.00	1.288	0.04493	66.976	4.316	1.5	158.6

<sup>a</sup>  $D = 6.5 \times 10^{-6}$  cm.<sup>2</sup>/sec. was used in the theoretical computations.



**Table VII**—Data Used for Theoretical Computations with Model 4<sup>a</sup>

Emulsion System Used, ml.	Oil Volume, ml.	C <sub>0</sub> * ml./ml.	E × 10 <sup>6</sup>	H × 10 <sup>5</sup>	P × 10 <sup>5</sup>	K
0.75	0.161	0.04493	1.331	9.63	1.5	158.6
1.50	0.322	0.04493	2.662	9.63	1.5	158.6
3.00	0.644	0.04493	5.324	9.63	1.5	158.6
6.00	1.288	0.04493	10.648	9.63	1.5	158.6

<sup>a</sup> D = 6.5 × 10<sup>-6</sup> cm.<sup>2</sup>/sec. was used in the theoretical computations.

### DISCUSSION

The present studies appear to be significant for a number of reasons. First, the very low permeability of the gelatin film at the oil-water interface is surprising. Cast films (10, 11) of hydrophilic polymers and polyelectrolytes are generally expected to be relatively

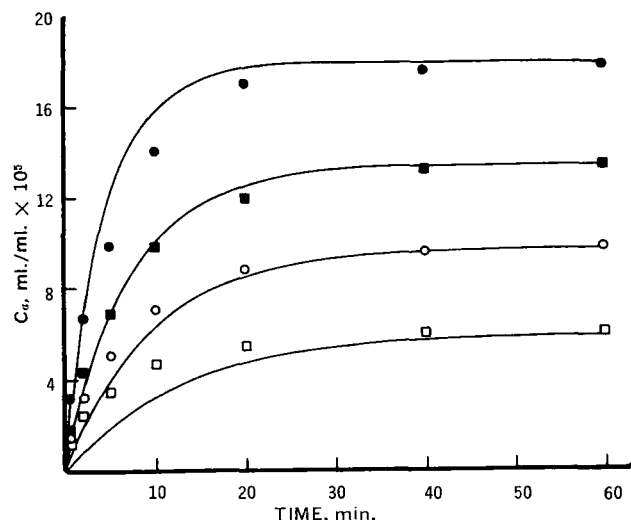


**Figure 14**—Comparison of experimental data with theory using Model 4. C<sub>a</sub> = amount of diethylphthalate released, ml./ml., versus time in minutes. Key: experimental points from System 1, □, 0.75 ml.; ○, 1.5 ml.; ■, 3.0 ml.; ●, 6.0 ml. Curves are theoretical values computed using Eqs. 9, 19a, 19b, and 22. Parameters used are shown in Tables IV and VII.

permeable to small molecular-weight solutes in aqueous media. Thus these results suggest that the hexadecane-gelatin interactions at the oil-gelatin interface must be particularly strong, giving rise to a very condensed film.

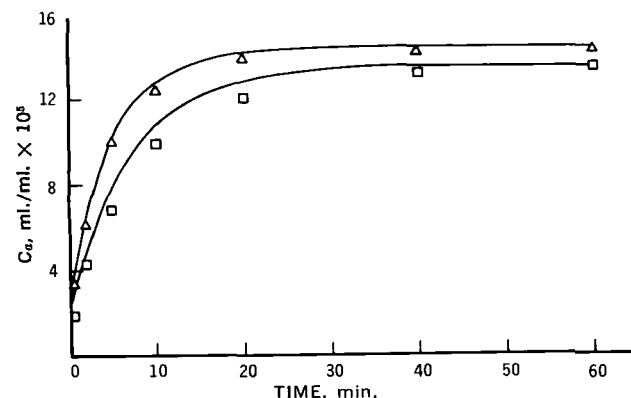


**Figure 15**—Comparison of the experimental data and theory using Model 3 for two different particle-size distribution systems. Key: experimental points, □, 3 ml. System 1; △, 3 ml. System 2. Curves are theoretical values computed using Eqs. 10-16.

The biological implication of these findings is that barriers of the magnitude observed here may easily govern the transport of drugs and other solutes in tissues and across membranes. As there is nothing obviously unique about the hexadecane-gelatin pair, one might expect interfacial barriers of comparable magnitude deriving from other combinations of an oil and a macromolecule (protein).

Such barriers, for example, may be associated with walls of the cells that make up a biological membrane such as the stratum corneum in percutaneous absorption or the barrier in intestinal absorption. It is noteworthy that the very low diffusion coefficient (10<sup>-9</sup> to 10<sup>-10</sup> cm.<sup>2</sup> sec.<sup>-1</sup>) observed by Scheuplein (12) for the stratum corneum is of the same order of magnitude expected from the data obtained in this research, assuming a reasonable composite membrane model and assuming that the cell walls of the stratum corneum have permeability characteristics of those for the gelatin-hexadecane interface.

The permeability coefficients of three algal species were recently reported (13-15) for some solutes and these are reproduced in Table VIII. It is interesting to note that the magnitudes for the permeability coefficients in Table VIII are of the order of magnitude observed in this study. Thus future studies employing the techniques developed here should prove to be very interesting in biology.

The present studies also appear to be significant from the standpoint of providing data that are accessible to physical model analyses. Thus four models differing in their physical assumptions were

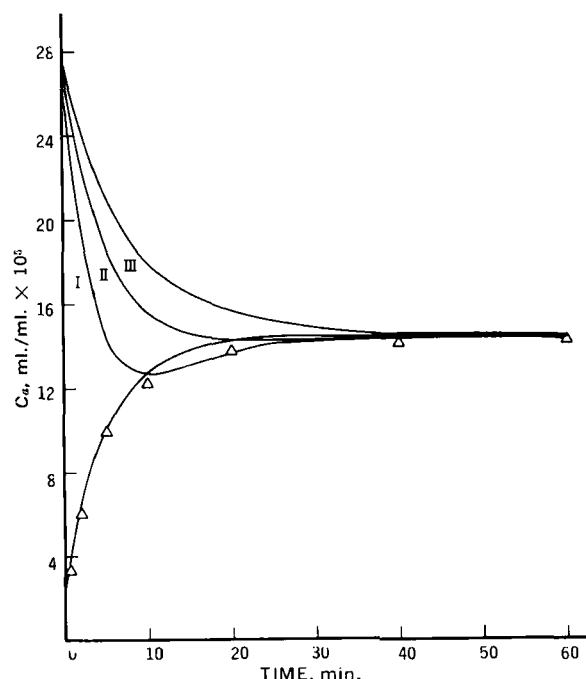


**Figure 16**—Theoretical calculation for the time dependence of the solute concentrations in the oil droplets of different sizes during a release experiment. Model 3 and Eqs. 10-16 were used. Key: △, experimental values of C<sub>a</sub> for the 3-ml. experiment using System 2. Lower curve is the theoretically calculated C<sub>a</sub> values. Upper curves are the computed C<sub>wi</sub> values as a function of time for three different particle sizes in the distribution. Curves I, II, and III are for droplets of radii 0.81μ, 1.45μ, and 2.15μ, respectively.

**Table VIII**—Permeability Coefficients of Some Algal Species

Solutes <sup>a</sup>	<i>Chara australis</i> , <sup>b</sup> P cm. sec. <sup>-1</sup>	<i>Nitella translucens</i> , <sup>b</sup> P cm. sec. <sup>-1</sup>	<i>Nitella mucronata</i> , <sup>c</sup> P cm. sec. <sup>-1</sup>
Urea <sup>d</sup>	—	$7.4 \times 10^{-7}$	—
Methanol	$2.94 \times 10^{-4}$	$2.85 \times 10^{-4}$	$3.2 \times 10^{-4}$
Ethanol	$1.97 \times 10^{-4}$	$2.72 \times 10^{-4}$	$3.0 \times 10^{-4}$
Isopropanol	$1.53 \times 10^{-4}$	$1.72 \times 10^{-4}$	$2.3 \times 10^{-4}$

<sup>a</sup> Measured with <sup>14</sup>C isotopes. <sup>b</sup> Reference 14. <sup>c</sup> Reference 15. <sup>d</sup> Reference 13.

compared to the data, and it was found that a permeability coefficient value of  $1.5 \times 10^{-5} \pm 0.3$  gave the best fit of the data to each of the models. While the effect of diethylphthalate binding was not large in the present instance, it must be accounted for (Model 3) in order to provide quantitative consistency. Furthermore the best model (Model 3) was that in which the bound solute was assumed to be in rapid equilibrium with the aqueous phase rather than with the oil phase. This is physically reasonable when one views the main barrier as primarily arising from the hexadecane-gelatin interactions and the outer portion of the gelatin film interacting with the aqueous phase as being somewhat swollen even in the presence of the salt concentration and therefore relatively permeable to solutes.

### GLOSSARY

$G_i$	= rate of solute release from a droplet $i$ .
$a_i$	= radius of the droplet $i$ .
$D$	= diffusion coefficient.
$P$	= permeability coefficient.
$K$	= oil-water partition coefficient.
$K'$	= apparent oil-water partition coefficient with adsorbed gelatin at the interface.
$C'$	= solute concentration just outside the adsorbed film on the aqueous side.
$C_{wi}$	= hypothetical aqueous solute concentration of oil droplet $a_i$ in equilibrium with $C_{oi}$ .
$C_{oi}$	= solute concentration in the oil droplet $a_i$ .
$V_{oi}$	= volume of a droplet $a_i$ .
$V_o$	= volume of the oil phase.
$n_i$	= number of the droplets with radii between $a_i$ and $a_{i+1}$ .
$V_a$	= volume of the aqueous phase.
$C_a$	= solute concentration in the aqueous phase.
$C_0^*$	= solute concentration in the oil phase at time equal to zero.
$E$	= expected solute concentration in the aqueous phase at time equal to zero when the contribution from interfacial desorption of the solute is ignored.
$E'$	= solute concentration in the aqueous phase at time equal to zero calculated using Eq. 12.

$t$	= time.
$\Delta t$	= time increment.
$\Delta C_{wi}$	= change in $C_{wi}$ during $\Delta t$ .
$Q$	= amount of diethylphthalate bound to the adsorbed gelatin prior to dilution of the emulsion in the medium.
$A(C_a, V_o)$	= amount of diethylphthalate bound at the interface.
$A(E', V_o)$	= amount of diethylphthalate bound at the interface at time equal to zero.
$C_{oi}^T$	= apparent concentration of the solute in the oil droplet of radius $a_i$ .
$f(C_{oi}, a_i)$	= contribution to $C_{oi}^T$ due to the bound solute.
$H$	= a constant and defined at Eq. 21.
$\Delta C_{oi}^T$	= change in $C_{oi}$ during $\Delta t$ .

### REFERENCES

- (1) R. J. Archer and V. K. LaMer, *J. Phys. Chem.*, **59**, 200 (1955).
- (2) T. J. Roseman, "Mechanism of Action of Interfacially Adsorbed Agents on the Demineralization Rate of Enamel," Ph.D. dissertation, University of Michigan, Ann Arbor, Mich., 1967.
- (3) A. H. Goldberg, W. I. Higuchi, N. F. H. Ho, and G. Zografi, *J. Pharm. Sci.*, **56**, 1432(1967).
- (4) S. G. Frank, "Micellar Solubilization of Water in Hydrocarbon Solvents," Ph.D. dissertation, University of Michigan, Ann Arbor, Mich., 1968.
- (5) C. W. N. Cumper and A. E. Alexander, *Trans. Faraday Soc.*, **46**, 235(1950).
- (6) A. H. Ghanem, W. I. Higuchi, and A. P. Simonelli, to be published.
- (7) N. F. H. Ho and W. I. Higuchi, *J. Pharm. Sci.*, **56**, 248 (1967).
- (8) W. I. Higuchi, *ibid.*, **56**, 315(1967).
- (9) *ibid.*, **53**, 405(1964).
- (10) H. P. Gregor and E. Kantner, *J. Phys. Chem.*, **61**, 1169 (1957).
- (11) R. H. Johnson, *J. Pharm. Sci.*, **54**, 327(1965).
- (12) I. H. Blank, R. J. Scheuplein, and D. J. Macfarlane, *J. Invest. Dermatol.*, **49**, 582(1967).
- (13) J. Dainty and B. Z. Ginzburg, *Biochim. Biophys. Acta*, **79**, 112(1964).
- (14) *ibid.*, **79**, 122(1964).
- (15) R. Collander, *Physiol. Plantarum*, **7**, 420(1954).

### ACKNOWLEDGMENTS AND ADDRESSES

Received July 24, 1968, from the College of Pharmacy, University of Michigan, Ann Arbor, MI 48104

Accepted for publication October 16, 1968.

Presented to Basic Pharmaceutics Section, APHA Academy of Pharmaceutical Sciences, Miami Beach meeting, May 1968.

This investigation was supported by grant GM-13368 from the National Institute of General Medical Sciences, U. S. Public Health Service, Bethesda, Md.